Journal of Peptide Science
J. Pept. Sci. 2006; **12**: 766–774
Published online in Wiley InterScience (www.interscience.wiley.com). DOI: 10.1002/psc.811

JOURNAL OF PEPTIDE SCIENCE

Exploring interaction of β-amyloid segment (25–35) with membrane models through paramagnetic probes

CINZIA ESPOSITO,[a] ANNAMARIA TEDESCHI,[a] MARIO SCRIMA,[a] GERARDINO D'ERRICO,[b] M. FRANCESCA OTTAVIANI,[c] PAOLO ROVERO[d] and ANNA MARIA D'URSI[a]*

[a] Dipartimento di Scienze Farmaceutiche, University of Salerno, 84084-Fisciano, Italy
[b] Dipartimento di Chimica, University of Napoli, Napoli, Italy
[c] Dipartimento di Chimica, University of Urbino, Urbino, Italy
[d] Dipartimento di Scienze Farmaceutiche, University of Firenze, Firenze, Italy

Received 28 July 2006; *Revised 2 October 2006*; *Accepted 2 October 2006*

Abstract: The accumulation of β-amyloid peptides into senile plaques is one of the hallmarks of Alzheimer's disease (AD). There is mounting evidence that the lipid matrix of neuronal cell membranes plays an important role in the β-sheet oligomerization process of β-amyloid. Aβ(25–35), the sequence of which is GSNKGAIIGLM, is a highly toxic segment of amyloid β (Aβ)-peptides, which forms fibrillary aggregates. In the present work, two spin-labelled Aβ(25–35) analogues containing the nitroxide group of the amino acid TOAC (2,2,6,6-tetramethylpiperidine-1-oxyl-4-amino-4-carboxylic acid) as a paramagnetic probe at the *N*- or the *C*-terminus of the peptide sequence, respectively, were synthesized in order to investigate the peptide-membrane interaction. The orientation and associated changes of the peptide conformation in the presence of different artificial membrane models (micelles, liposomes) were evaluated by electron paramagnetic resonance and circular dichroism techniques. The results of this study allowed us to propose a model in which the *C*-terminal portion of the peptide is highly associated to the membrane, while the *N*-terminal part extends into the aqueous phase with occasional contacts with the lipid head-group region. Interestingly, the interaction of the *C*-terminal portion of the peptide is particularly enhanced in the presence of sodium dodecyl sulfate (SDS) molecules. Copyright © 2006 European Peptide Society and John Wiley & Sons, Ltd.

Keywords: β-amyloid(25–35); electron paramagnetic resonance; liposomes; micelles

INTRODUCTION

The Aβ-amyloid peptides are the major constituents of senile plaques in AD [1–3]. A great deal of evidence indicates that the Aβ-amyloid peptides, in the form of soluble β-sheet oligomers, are highly toxic and directly involved in the pathogenesis of AD [4]. The Aβ-amyloid peptides are peculiarly susceptible to conformational transitions from random-coil or α-helical structure, in which they preferentially are in the nontoxic monomeric form, to β-sheet structure, in which they associate to form oligomers, responsible for the peptide neurotoxicity [5]. Many factors of different nature are able to modulate the amyloid conformation, enhancing or blocking the β-sheet oligomerization process. Cellular interfaces are reported to affect the aggregation rates and even the structures of the aggregates [6–8]. Sphingolipid- and cholesterol-rich bilayer membranes known as *lipid rafts* appear to be especially important sites of Aβ aggregation because the α- and β-secretases that generate the Aβ peptides from amyloid precursor proteins (APPs) as well as the Aβ peptides themselves are concentrated in lipid rafts [9,10].

It has been proposed that Aβ(25–35) represents the biologically active region of Aβ amyloid because it represents the shortest fragment that exhibits large β-sheet aggregated structures and retains the toxicity of the full-length peptide [11,12]. Several reports have also indicated that Aβ(25–35), in a manner similar to that of Aβ(1–42), undergoes a conformational transition from a soluble, random-coil form to aggregated fibrillary β-sheet structures, depending on the environmental conditions.

In the last few years, EPR techniques have been developed and successfully applied to obtain important structural and dynamical information on membrane-associated peptides. Site-directed spin labeling involving nitroxide radicals as spin probes has been the most frequently used EPR technique applied to biologically relevant systems [13–18]. In particular, the

Abbreviations: Alzheimer's disease, (AD); amyloid β, Aβ; circular dichroism; CD, cholesterol, CHOL; critical micellar concentration, cmc; N,N′-diisopropylethylamine, DIEA; *N*,*N*-dimethylformamide, DMF; dodecylphosphocholine, DPC; DL-α-phosphatidylcholine dipalmitoyl, DPPC; 1,2-dipalmitoyl-sn-glycero-3-phosphate sodium salt, DPPG; electron paramagnetic resonance, EPR; electrospray ionization-mass spectroscopy, ESI-MS; 9-fluorenylmethoxycarbonyl, Fmoc; *O*-(benzotriazol-1-yl)-1,1,3,3-tetramethyluronium hexa-fuorophosphate, HBTU; 1-hydroxybenzotriazole, HOBt; mutilamellar vesicles, MLVs; room temperature, RT; sodium dodecyl sulfate, SDS; sphingomyelin, SPM; small unilamellar vesicles, SUVs; tBu, tert-butyl; trifluoroacetic acid, TFA; triisopropylsilane, TIS; 2,2,6,6-tetramethylpiperidine-1 oxyl-4-amino-4-carboxylic acid, TOAC.

*Correspondence to: A. M. D'ursi, Dipartimento di Scienze Farmaceutiche, Università di Salerno, Via Ponte Don Melillo 11C, 84084 Salerno, Italy; e-mail: dursi@unisa.it

nonproteinogenic amino acid TOAC has been successfully used. The nitroxide radical is part of the rigid piperidine ring, whose carbon atom at the 4th position represents the C^{α} atom of the amino acid itself [19].

In this work, we strategically introduced the spin label TOAC into the Aβ(25–35) peptide sequence at either the *N*-terminus or the *C*-terminus site [20]. Useful dynamical and structural information were extracted from the computer aided analysis of the EPR spectra of the spin-labelled peptides in different membrane-mimicking systems as micelles and liposomes. Conformational changes in the peptide structure were observed by using CD.

MATERIALS AND METHODS

Peptide Synthesis

The Aβ(25–35) amyloid peptide, GSNKGAIIGLM, and the TOAC labeled derivatives, Ac-^{24}TOAC-GSNKGAIIGLM, designated as Aβ–TOAC^{NTerm}, and GSNKGAIIGLM-^{36}TOAC-^{37}G, designated as Aβ–TOAC^{Cterm}, were manually synthesized by conventional solid-phase chemistry using the Fmoc/tBu strategy [21]. The Fmoc-TOAC-OH and the subsequent amino acid in sequence were doubly coupled using HOBt and HBTU (fourfold excess) as coupling reagents. Peptide–resin cleavage and side chain deprotection reactions were carried out in 90% TFA, 5% water, and 5% TIS. The resin was filtered, and the solution added drop wise to cold tert-butylmethyl ether in order to precipitate the peptide. To re-oxide the spin label back to the nitroxide form, both the TOAC labeled peptides were treated with 10% aqueous ammonia (pH 9.5) for 4 h at room temperature before and after HPLC purification [22,23].

HPLC Purification

Analytical HPLC was carried out on a System Gold 125s model (Beckmann Coulter) equipped with a UV166 detector. Preparative HPLC was carried out on a Waters 600E system controller equipped with a 486 UV detector. A Jupiter (Phenomenex) C18 column (25 × 4.6 cm, 5 μ, 300 A° pore size) was used for analytical runs and a Vydac C18 column (25 × 10 cm, 5μ, 300 A° pore size) was used for peptide purification. Analytical separations were performed with a linear gradient (5–50% in 45 min) of CH_3CN in water containing 0.1% TFA. Flow rate: 1 ml/min. UV detection: 210 nm.

Mass Spectra Analysis

All the peptides were characterized on a Finningan LCQ-Deca ion trap instrument equipped with an electrospray source (LCQ Deca Finnigan, San José, CA, USA); samples were directly infused in the ESI source by using a syringe pump at a flow rate of 5 μl/min. Data were analyzed with Xcalibur software.

Sample Preparation

Stock aqueous solutions were prepared for both Aβ-TOAC^{Nterm} and Aβ-TOAC^{Cterm} and diluted to a final concentration of 0.01 mM. This solution was used as solvent for preparing micellar aqueous mixtures to be investigated by both EPR and CD spectroscopies.

Micellar solutions were prepared at a surfactant concentration well above the critical micelle concentration. Concerning the pure micelle solutions, the chosen concentration for SDS is 0.1 M and for DPC is 0.1 M; concerning the mixture SDS/DPC, the chosen total surfactant molarity is 0.1 M, and the ratio between the surfactant concentrations M_{SDS}/M_{DPC} is equal to 30/70. The concentration of spin-labeled peptides is low enough to ensure that a maximum of one radical can interact with each micellar aggregate, thus avoiding spin exchange between different spin-labelled molecules.

Preparation of SUVs

SUVs were prepared by dissolving the phospholipids in the absence or in the presence of CHOL and SPM in chloroform/methanol (50/50), and then removing the solvent with a rotary evaporator by evaporation for at least 3 h under high vacuum at room temperature. The dry lipid films were then re-suspended in 0.01 mM spin-labelled peptide aqueous solution at a temperature above the gel-liquid crystal transition temperature. After vigorous shaking, disruption of MLV suspensions by sonic energy gave the desired SUVs.

The SUVs were composed of DPPG/DPPC (80/20 molar ratio), DPPG/DPPC/CHOL (60/15/25 molar ratio), and DPPG/DPPC/CHOL/SPM (50/12.5/25/12.5). Samples were prepared in such a way that the peptide/SUV molar ratio was 1/20.

Circular Dichroism

CD spectra were performed on an 810-Jasco spectropolarimeter at room temperature, using a quartz cuvette with a path length of 1 mm. The spectra were the average of ten accumulations from 190 to 260 nm, and recorded with a bandwidth of 1 nm at a scanning speed of 50 nm/min. All the spectra were analyzed, subtracted by blanks, and finally corrected by smoothing. The estimation of the secondary structure composition was carried out using the algorithm K2D by DichroWeb [24].

EPR Measurements

The EPR spectra were recorded by means of a Bruker ELEXYS e500 X-band spectrometer at a microwave frequency of 9.45 GHz. The EPR spectrometer parameters were as follows: modulation amplitude, 0.16 G (to avoid signal over modulation); time constant, 40.96 ms; receiver gain, 60 dB; attenuation, 20 dB (to prevent saturation effects). All measurements were performed at RT. The accumulation and the gain were varied in each measurement in order to optimise the spectrum. Since we showed that the presence of oxygen in solutions could modify the EPR line-width, they were saturated with nitrogen and successively sealed in 1.00 mm i.d. quartz capillaries.

EPR Spectra Calculations

The analysis of the EPR spectra was carried out by means of the simulation program by Freed and coworkers [25,26],

DOI: 10.1002/psc

which takes into account the relaxation process of the nitroxides. The main parameters extracted from the spectral analysis are (i) the A_{zz} component of the coupling tensor between the electron spin and the ^{14}N nuclear spin, **A**, whose increase is related to an increase in environmental polarity of the radicals and (ii) the τ_{perp} perpendicular component of the correlation time associated to the rotational diffusion motion of the probe (the Brownian diffusion ($D_i = 1/(6\tau_i)$) model was used in the computation). In some cases, the spectra were constituted by two components. Each component was obtained by subtracting the single component of the spectrum from the spectrum relative to the combined components. Then, each component was computed to extract the parameters that were informative of the mobility and structural variations of the label. The accuracy of the parameters (2–5%) was determined by computations: a larger than 2–5% variation of a parameter led to a perceptible variation of the computed line shape and, consequently, to a worse fitting between the computed and the experimental spectra. Since different sets of parameters could provide an equivalent or even better fitting between the experimental and the computed line shapes after several attempts of computations, the ones reported in this study are the most confident for the physical meaning of the systems. However, a high degree of confidence of the reported parameters (accuracy of 2%) allows us to estimate the microenvironmental variations in correspondence of variations to the 1st or 2nd decimal in the parameters. In these last cases, we assume that no other sets of parameters provide a better fitting.

RESULTS

EPR Analysis

The EPR spectra of the two spin-labelled peptides in aqueous solution were compared with that of the TOAC molecule by means of computation of the line shape. Figure 1 shows the experimental and computed spectra. Table 1 reports the main parameters obtained from computation (A_{zz} and τ_{perp}, accuracy 2%) for the three probes TOAC, Aβ-TOAC^{Nterm}, and Aβ-TOAC^{Cterm}.

No significant difference between Aβ-TOAC^{Nterm} and Aβ-TOAC^{Cterm} was found in the spectral signals reported in Figure 1(b) and (c), respectively.

The A_{zz} values indicated a polar environment accounted by the label hydration. It is interesting to observe that the spin-labelled peptides show a lower A_{zz} than the TOAC molecule, suggesting that the nitroxide radical in the spin-labelled peptides experiences a reduced polar environment than water. This evidence suggests that the nonpolar R groups of the peptide partially shield the TOAC residue from water molecules.

It is evident from the τ_{perp} values that the incorporation into different peptides leads to a significant reduction in the flexibility of the TOAC moiety (τ_{perp} increases from ~0.08 ns, for TOAC, to ~0.20 ns, for the labeled peptides) because its mobility reflects the mobility of the peptide. However, the τ_{perp} remains in the fast motion regime, suggesting that the peptides tend to assume an unordered structure.

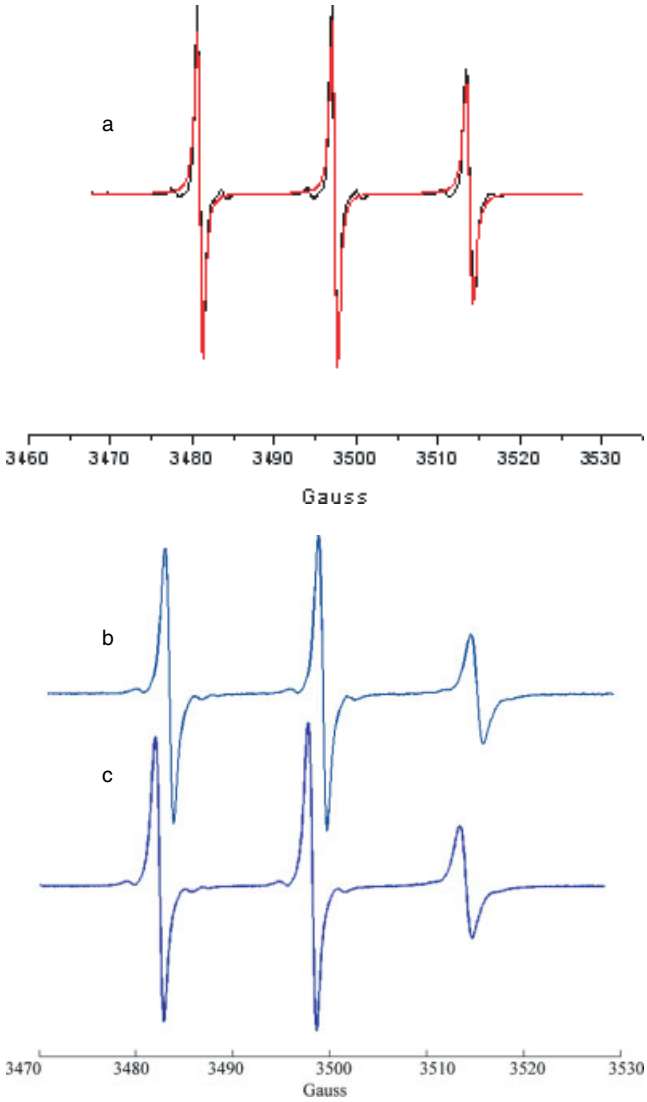

Figure 1 (a–c) Experimental (–) and calculated (–) EPR spectra, respectively, of TOAC molecule, Ab-TOAC^{Nterm}, and Aβ-TOAC^{Cterm} spin-labeled peptides performed in water at RT.

Interaction of Aβ(25–35) with micelles. The EPR spectra were recorded on the Aβ (25–35) peptide spin-labeled with TOAC at the *C*-terminus and at the *N*-terminus, Aβ-TOAC^{Cterm}, and Aβ-TOAC^{Nterm}, respectively, in SDS and DPC micellar solutions, as well as in the SDS/DPC (30/70 molar ratio) mixture. We analyzed the spectral pattern modifications induced by the interaction of the Aβ-peptide with micelles.

From the spectral analysis carried out by the simulation procedure, it resulted that the EPR spectra of the Aβ-TOAC^{Nterm} and Aβ-TOAC^{Cterm} in the presence of the micelles show the superposition of two signals: (i) the isotropic three line signal characteristic of the free probes in water (this component is henceforth called "free component") and (ii) a slow motion spectrum that shows resolution of the anisotropic components of the magnetic tensors, as usually found for probes feeling a high viscosity microenvironment (this component

DOI: 10.1002/psc

Table 1 Main Parameters Obtained from Computation of the EPR Signals of TOAC Molecule, Aβ-TOAC^{Nterm}, and Aβ-TOAC^{Cterm} Spin-labelled Peptides Measured in All the Examined Systems at RT

SAMPLE	$\tau_{perp}/10^{-10}$ S (free component)[a]	A_{zz}/G (free component)[a]	$\tau_{perp}/10^{-10}$ S (interacting component)[b]	A_{zz}/G (interacting component)[b]
TOAC	0.83	37.40	—	—
Aβ-TOAC^{Nterm} in water	2.17	36.90	—	—
Aβ-TOAC^{Nterm} in SDS	2.48	36.85	Not measurable	Not measurable
Aβ-TOAC^{Nterm} in DPC	2.10	36.90	Not measurable	Not measurable
Aβ-TOAC^{Nterm} in SDS/DPC	2.64	36.83	20.5	35.5
Aβ-TOAC^{Cterm} in water	2.50	36.90	—	—
Aβ-TOAC^{Cterm} in SDS	Not measurable	Not measurable	24	36.5
Aβ-TOAC^{Cterm} in DPC	2.53	36.85	Not measurable	Not measurable
Aβ-TOAC^{Cterm} in SDS/DPC	2.62	36.90	31	36.0

[a] Accuracy, 2%, on the basis of computation.
[b] Accuracy, 3%, on the basis of computation.

is henceforth called 'interacting component' and is attributed to labeled peptides interacting with the micelle surface). The two components were analyzed separately using a simulation procedure so that parameters informative of the mobility and structural variations of both Aβ-TOAC^{Nterm} and Aβ-TOAC^{Cterm} were obtained. The uncertainty of the parameters that resulted from spectral computation (Table 1) is low for the free component (2%, when this component is extracted by subtracting the interacting component from the experimental signal), whereas it increases to 3–4% for the interacting component.

The presence of two components in the spectra is due to the distribution of the labels in two environments, which can be in contact with the micelles (interacting component) and far from the micelle surface (free component) in slow exchange in the EPR timescale (10^{-8} s). This means that the peptide–micelle interactions are strong enough to increase the 'permanence time' of the peptides in contact with the micelles, but a fraction of peptides remains free since shielded by the interacting peptides, or due to a saturation of the interacting capability of the micelles. Therefore, a lower amount of free labels indicates a lower interacting capability of the micelles.

In all the examined micellar systems, a larger amount of the free component was found for Aβ-TOAC^{Nterm} compared to Aβ-TOAC^{Cterm}. In the case of Aβ-TOAC^{Nterm}, the major spectral component corresponds to a highly mobile spin probe, indicating that the *N*-terminus of the Aβ-peptide undergoes rapid rotation. This finding suggests that the *N*-terminus portion of the peptide is less involved in the interaction with the micelles.

In Figure 2, we report the spectra of Aβ-TOAC^{Cterm} in water, in pure SDS and pure DPC micelles, and in SDS/DPC mixed micelles. In Figure 3, an example of the simulation procedure is shown. In particular, the experimental and calculated spectra of Aβ-TOAC^{Cterm}

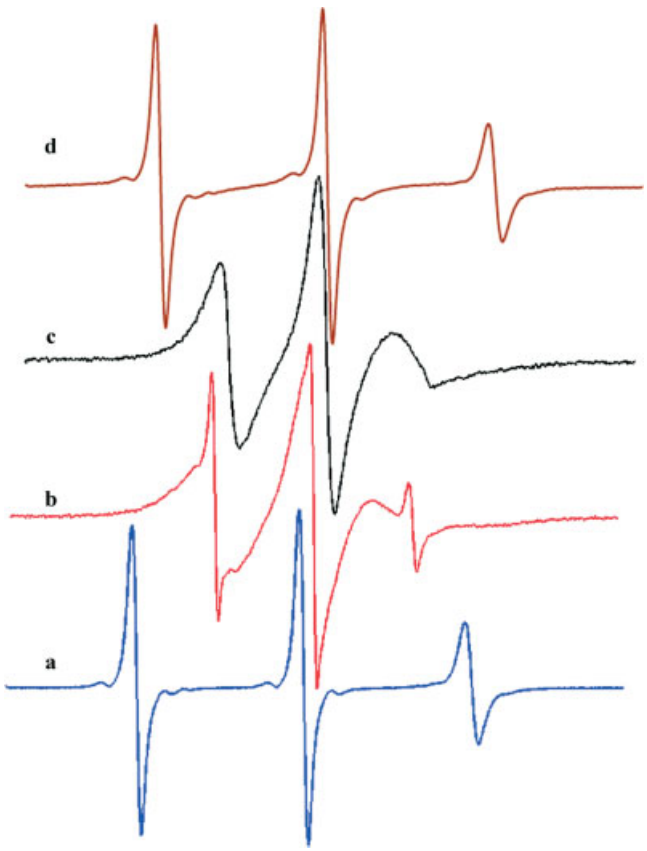

Figure 2 Experimental EPR spectra of Aβ-TOAC^{Cterm} recorded in water (a); in SDS/DPC mixed micelles (b); in SDS pure micelles (c); and in DPC pure micelles (d).

recorded in SDS/DPC are reported; the computed lines (red lines) are superimposed on the experimental lines. The experimental interacting component is obtained by subtracting the free component (probe in solution) from the total spectra.

The free component is predominant in pure DPC micelles (80%), it becomes less evident in SDS/DPC

DOI: 10.1002/psc

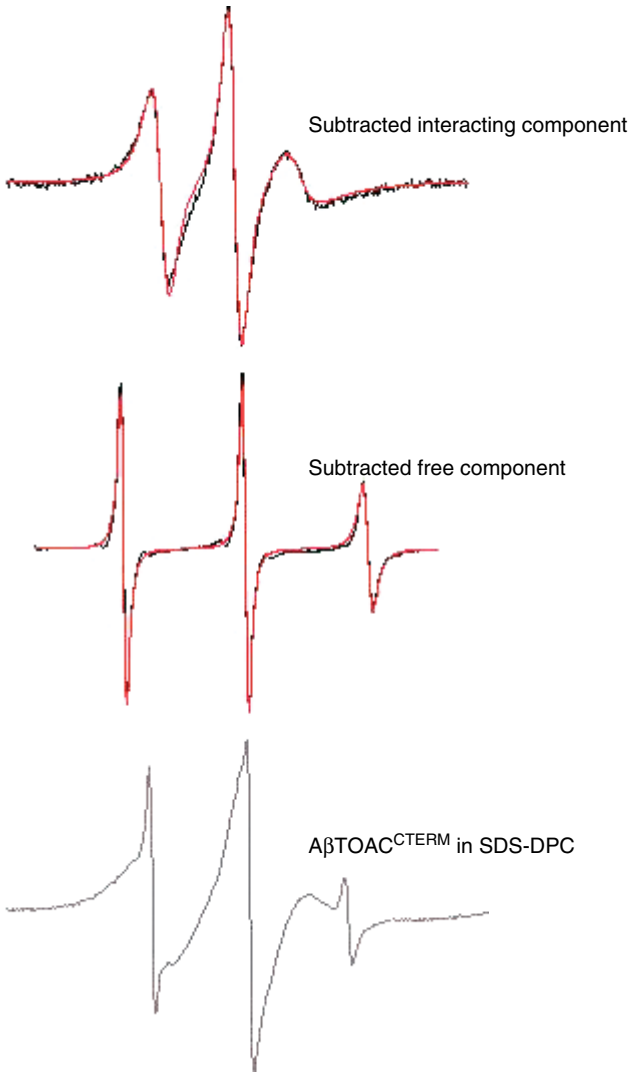

Figure 3 Experimental (–) and calculated (–) EPR spectra Aβ-TOAC^{Cterm} recorded in SDS/DPC with subtracted interacting and subtracted free components.

mixed micelles (38%) and turns out to be almost absent for the spectrum in pure SDS micelles. Taken together, these data indicate that Aβ(25–35) peptide preferentially interacts with anionic micelles involving its *C*-terminal portion. Moreover, the peptide–micelle interaction is shown to be mainly electrostatically driven.

On the other hand, the τ_{perp} values (Table 1) show that the interacting component is different with respect to the mobility conditions for the two systems, SDS and SDS/DPC. The interacting component for the DPC systems is not computable owing to the too low intensity, but a visual inspection indicates a faster rotational mobility with respect to the SDS system. We found that the mobility of the *C*-terminus labeled peptide is lower when interacting with the mixed micelles, as compared to the SDS micelles (stronger interactions with the SDS/DPC mixed micelles when compared to the SDS micelles). This finding suggests that once the peptide has established the electrostatic interaction with the SDS molecules, binding also occurs between the peptide residues and the DPC molecules.

These results indicate that the Aβ(25–35) peptide preferentially binds to the micelles via the *C*-terminal part. The driving force of the peptide-micelles interaction is predominantly electrostatic, but it also shows a hydrophobic contribution.

Interaction of Aβ(25–35) with liposomal systems. We recorded the spectra of Aβ-TOAC^{Nterm} and Aβ-TOAC^{Cterm} in SUVs constituted by DPPG/DPPC (80/20 molar ratio), SUVs containing cholesterol (SUVs/CHOL), and SUVs containing cholesterol and sphingomyelin (SUVs/CHOL/SPM).

The EPR spectra of Aβ-TOAC^{Nterm} and Aβ-TOAC^{Cterm} in SUVs are generally similar to the spectra in water. However, some interesting differences, which are obtained from the analysis of the spectra and the computation of the spectral line shape, are apparent.

The computed EPR spectral parameters of Aβ-TOAC^{Nterm} in the DPPG/DPPC SUVs are reported in Table 2. The spectrum of the label is similar to that in water. A different situation was found for Aβ-TOAC^{Cterm}: for the DPPG/DPPC SUVs, both a free and an interacting component contribute to the spectrum. The interacting component is anyway a single-line spectrum, as shown in Figure 4(a), arising from spin–spin exchange narrowing, which occurs at high local concentrations of radical groups. Therefore, self-aggregation of a portion of labeled peptides takes place, which is attributed to the condensation of the peptides interacting with the liposome surface. The free component in this case is similar to that in water solution.

The evidence suggest, as found for the micellar systems, that the Aβ(25–35) peptide interacts with liposomal systems, with the *C*-terminus part condensing at the liposome surface and being hosted in the hydration layer of the liposome, whereas the *N*-terminus part extends in the surrounding aqueous medium.

When cholesterol is added to the SUVs, the Aβ-TOAC^{Nterm} shows a decrease in the correlation time (Table 2). Addition of SPM does not cause any further change in the spectral parameter. Therefore when CHOL or CHOL/SPM is present, the most interesting feature is that the mobility of the labeled peptide, in particular the *N*-terminal part, is higher in the presence of liposome solution than in water. Therefore, the *N*-terminus of the peptide gains freedom when the SUV/CHOL or the SUV/CHOL/SPM liposomes are present. In the meantime, the A_{zz} value decreases. These results are explained on the basis of a variation of the peptide structure in solution when the packed SUV/CHOL liposomes are present: a low ordered peptide structure well accounts for both the increased mobility and decreased polarity of Aβ-TOAC^{Nterm}. Also,

DOI: 10.1002/psc

Table 2 Main Parameters Obtained from Computation of the EPR Signals of Aβ-TOAC^{Nterm} and Aβ-TOAC^{Cterm} Spin-labelled Peptides Measured in SUVs at RT

SAMPLE	$\tau_{perp}/10^{-10}$ S (free component)[a]	A_{zz}/G (free component)[a]	$\tau_{perp}/10^{-10}$ S (interacting component)	A_{zz}/G (interacting component)
Aβ-TOAC^{Nterm} in SUVs	2.20	36.90	—	—
Aβ-TOAC^{Nterm} in SUVs-CHOL	1.81	36.80	—	—
Aβ-TOAC^{Nterm} in SUVs/CHOL/SPM	1.81	36.80	—	—
Aβ-TOAC^{Cterm} in SUVs	2.96	36.90	Not measurable	Not measurable
Aβ-TOAC^{Cterm} in SUVs/CHOL	2.54	36.85	—	—
Aβ-TOAC^{Cterm} in SUVs/CHOL/SPM	2.67	36.75	—	—

[a] Accuracy, 2%, on the basis of computation.

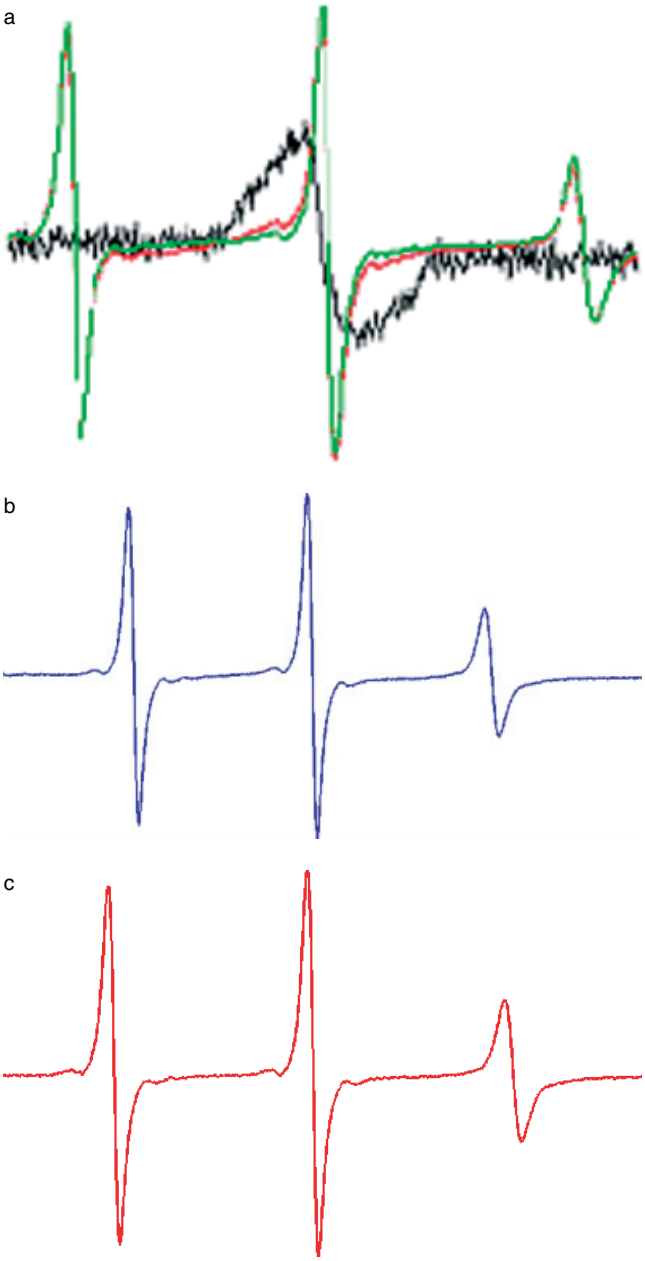

Figure 4 EPR spectra of Aβ-TOAC^{Cterm} recorded in SUVs (a), in SUVs/CHOL (b), and in SUVs/CHOL/SPM (c).

for Aβ-TOAC^{Cterm} the mobility evaluated from spectral computation (Figure 4(b) and (c)) increases by adding CHOL to the SUV liposomes, but this mobility remains lower than in water and the polarity decreases (Table 2). In this case, only the free component is present, and the labeled peptides do not show an electrostatic interaction with the liposome surface. This evidence suggests that by adding CHOL and SPM to the SUVs, the different packing of the phospholipids reduces and modifies the interaction of the peptide with the lipidic system, which in turn affects the peptide structure.

Circular Dichroism

CD experiments of the Aβ(25–35) amyloid fragment were aimed to follow the conformational changes associated to the peptide/membrane interaction.

CD spectra were recorded under the same conditions on the native peptide as well as on the spin-labeled peptides. Water solution, DPC/SDS mixed micelles, and pure SDS micelles as well as SUVs containing different components were used as solvents for native and labeled peptides.

The shapes of the CD spectra appear to be sensitive to the presence of membrane environment whereas they are not significantly affected by the presence of the TOAC moieties.

Figure 5 shows that CD spectrum of the Aβ(25–35) amyloid peptide in the aqueous medium is typical of a peptide characterized by unordered structures. On the contrary, in the presence of all the differently charged micelles, the CD curves indicate an appreciable presence of turn helical structures. Thus, the presence of the hydrophobic environment seems to favor a more ordered conformation with respect to the aqueous environment. In particular, an increasing extent of helical structure is observed in SDS and DPC micellar solutions (Panel A).

As it is observable from the comparison of panel A and B (Figure 5), moving from micelles to SUVs containing partially negative phospholipids, the Aβ(25–35) amyloid peptide preserves the propensity to be more structured

DOI: 10.1002/psc

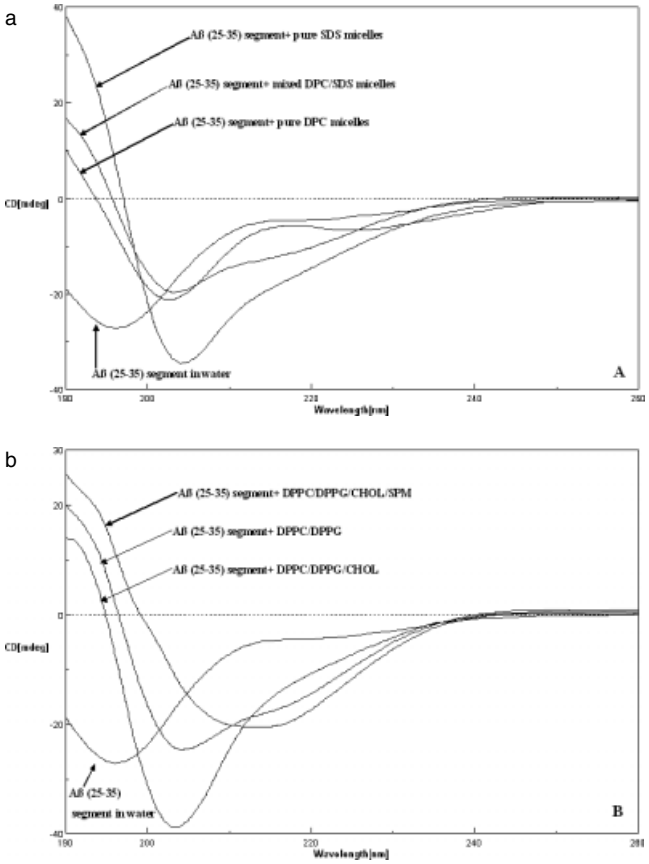

Figure 5 Panel A: CD spectra of the Aβ(25–35) peptide recorded in water, in pure SDS or DPC micelles and in mixed SDS/DPC micelles. Panel B: CD spectra of Aβ (25–35) recorded in water, in SUVs made up by the following compositions: DPPC/DPPG, DPPC/DPPG/CHOL, DPPC/DPPG/CHOL/SPM.

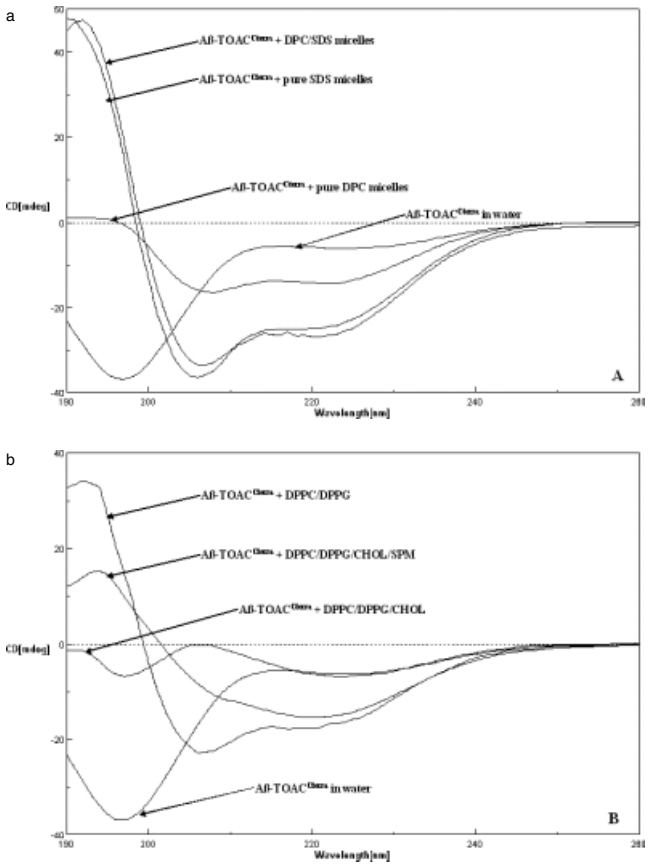

Figure 6 Panel A: CD spectra of the Aβ-TOAC^{Cterm} peptide recorded in water, in pure SDS or DPC micelles and in mixed SDS/DPC micelles. Panel B: CD spectra of Aβ-TOAC^{Cterm} recorded in water, in SUVs made up by the following compositions: DPPC/DPPG, DPPC/DPPG/CHOL, DPPC/DPPG/CHOL/SPM.

in membrane environment. However, the addition of the amount of CHOL typical of lipid raft composition in SUVs decreases the helical content of the peptide. Interestingly, a transition of the peptide from the α-helical to the β-sheet structure in the presence of both CHOL and SPM typical of the lipid raft composition is clearly observable.

Figure 6 shows that the solution conformation of Aβ-TOAC in water and in the presence of both micelles (panel A) and liposomes (panel B) closely resembles that of the unlabeled peptide, demonstrating that binding of TOAC to the peptide *C*-terminus has little effect on its conformational properties.

DISCUSSION

AD is characterized by the presence of a large number of fibrillar amyloid deposits in the form of senile plaques in the brain [1–3]. A wealth of experimental evidence provides support to the notion that the amyloid fibril assembly and the toxicity of pre-fibrillar aggregates are closely related and are both intimately membrane-associated phenomena [27–29]. In order to investigate the dynamics of interaction between amyloid and the membrane, we labeled the Aβ(25–35) fragment of β-amyloid with the TOAC paramagnetic probe, either at the *N*- or at the *C*-terminus, thus obtaining the Aβ-TOAC^{Nterm} and Aβ-TOAC^{Cterm} peptides, respectively. The Aβ(25–35) amyloid segment represents a suitable model of the full-length peptide because it is more manageable and preserves the peculiar features of the entire sequence in terms of aggregation and conformation [30,31]. TOAC labeling at the two extremities of the peptide provides an interesting tool to obtain clear information on the positioning of the peptide with respect to the membrane [9–16]. In the initial part of this study, we investigated the contribution of electrostatic and hydrophobic components as driving forces in the peptide/membrane interaction, employing differently charged micelles as SDS and DPC. Although SDS surfactant is often viewed as a denaturant that destroys native protein conformation, it provides a suitable anionic micellar interface [32,33], while DPC reproduces a zwitterionic

DOI: 10.1002/psc

environment [34]. Furthermore, a DPC micellar solution co-added with 30% SDS was prepared in order to mimic the partial negative charge of biological membranes.

The *N*-terminus of Aβ(25–35) is very flexible and exposed toward aqueous medium, indicating that it weakly interacts with micelles. On the contrary, the *C*-terminal part of Aβ(25–35) is immobilized onto the micelle surface. In particular, the EPR data show that a low fraction of the peptide is involved in the interaction with the zwitterionic SDS/DPC micelles, whereas a predominant fraction of the peptides interacts with the anionic micelles.

These findings are supported by CD experiments, which evidence that, in general, the presence of micelles stabilizes the Aβ(25–35) peptide in an α-helical structure.

This initial study supports the involvement of both electrostatic and hydrophobic contributions to the peptide–micelle interaction.

Moving from micelles to liposomes, the contributions of the chemical composition and membrane structural components, such as lipids, CHOL, and SPM, in affecting the interaction were evaluated.

In general, the Aβ(25–35) peptide interacts with liposome SUVs as with micellar systems. In particular, the EPR data show that the *C*-terminal part condenses at the liposome surface, whereas the *N*-terminus part extends away from the surface.

It is interesting to note that the interaction between Aβ(25–35) and the negatively charged phospholipids is weaker with respect to that between Aβ(25–35) and SDS micelles. This difference in behavior could be ascribed to the highly negative density charge of the sulfate head-group in the SDS surfactant [35].

Furthermore, our data indicate that the presence of SUVs encourages a peptide–peptide interaction, not appreciable in micelles, suggesting that the membrane bilayer structure is also important.

SUVs containing a 15–30 molar percent of CHOL, in the presence or absence of SPM, present a more rigid packing of the phospholipids bilayer. This effect discourages the peptide interaction with the aggregate [36,37]. The release of the peptide from the membrane surface is accompanied by a conformational change in the peptide structure, which becomes rich in β-sheet content, as shown by CD experiments. These results highlight that not only the physicochemical characteristics of a membrane, such as phase state, bilayer curvature, and surface charge, but also the particular chemical nature of the components are able to affect and modulate peptide structure and dynamics. In particular, we demonstrated that the presence of liposomes containing substantial amounts of CHOL and SPM, which is typical of lipid rafts, seems to favor the β-sheet oligomerization process of the amyloid peptide.

REFERENCES

1. Cohen AS, Calkins E. Electron microscopic observation on a fibrous component in amyloid of diverse origins. *Nature* 1959; **183**: 1202–1203.
2. Glenner GG, Wong CW. Alzheimer's disease: initial report of the purification and characterization of a novel cerebrovascular amyloid protein. *Biochem. Biophys. Res. Commun.* 1984; **120**: 885–890.
3. Miller DL, Papayannopoulos IA, Styles J, Bobin SA, Lin YY, Biemann K, Iqbal K. Peptide compositions of the cerebrovascular and senile plaque core amyloid deposits of Alzheimer's disease. *Arch. Biochem. Biophys.* 1993; **301**: 41–52.
4. Ikonomovic MD, Uryu K, Abrahamson EE, Ciallella JR, Trojanowski JQ, Lee VM, Clark RS, Marion DW, Wisniewski SR, DeKosky ST. Alzheimer's pathology in human temporal cortex surgically excised after severe brain injury. *Exp. Neurol.* 2004; **190**: 192–203.
5. Tomaselli S, Esposito V, Vangone P, van Nuland NA, Bonvin AM, Guerrini R, Tancredi T, Temussi PA, Picone D. The α-to-β conformational transition of Alzheimer's Aβ-(1–42) peptide in aqueous media is reversible: a step-by-step conformational analysis suggests the location of β conformation seeding. *Chembiochem* 2006; **7**: 257–267.
6. Zhao H, Tuominem EKJ, Kinnunen PKJ. Formation of amyloid fibers triggered by phosphatidylserine-containing membranes. *Biochemistry* 2004; **43**: 10302–10307.
7. Stefani M, Dobson CM. Protein aggregation and aggregate toxicity: new insights into protein folding, misfolding diseases and biological evolution. *J. Mol. Med.* 2003; **81**: 678–699.
8. Gorbenko GP, Kinnunen PKJ. The role of lipid-protein interactions in amyloid-type protein fibril formation. *Chem. Phys. Lipids* 2006; **141**: 72–82.
9. Kawarabayashi T, Shoji M, Younkin LH, Wen-Lang L, Dickson DW, Murakami T, Matsubara E, Abe K, Ashe KH, Younkin SG. Dimeric amyloid β protein rapidly accumulates in lipid rafts followed by apolipoprotein E and phosphorylated tau accumulation in the Tg2576 mouse model of Alzheimer's disease. *J. Neurosci.* 2004; **24**: 3801–3809.
10. Kokubo H, Saido TC, Iwata N, Helms JB, Shinohara R, Yamaguchi H. Part of membrane-bound Aβ exists in rafts within senile plaques in Tg2576 mouse brain. *Neurobiol. Aging* 2005; **26**: 409–418.
11. D'Ursi AM, Armenante MR, Guerrini R, Salvadori S, Sorrentino G, Picone D. Solution structure of amyloid beta-peptide (25–35) in different media. *J. Med. Chem.* 2004; **47**: 4231–4238.
12. Wei G, Shea JE. Effects of solvent on the structure of the Alzheimer amyloid-β(25–35) peptide. *Biophys. J.* 2006; **91**: 1638–1647.
13. Marsh D. Application of electron spin resonance for investigating peptide–lipid interactions, and correlation with thermodynamics. *Biochem. Soc. Trans.* 2001; **29**: 582–589.
14. Arbuzova A, Murray D, McLaughlin S. MARCKS, membranes, and calmodulin: kinetics of their interaction. *Biochim. Biophys. Acta* 1998; **1376**: 369–379.
15. Dempsey CE. The actions of melittin on membranes. *Biochim. Biophys. Acta* 1990; **1031**: 143–161.
16. Hubbell WL, Cafiso DS, Altenbach C. Identifying conformational changes with site-directed spin labelling. *Nat. Struct. Biol.* 2000; **7**: 735–739.
17. Millhauser GL. Selective placement of electron spin resonance spin labels: new structural methods for peptides and proteins. *Trends Biochem. Sci.* 1992; **17**: 448–452.
18. Ottaviani MF, Jockusch S, Turro NJ, Tomalia DA, Barbon A. Interactions of dendrimers with selected amino acids and proteins studied by continuous wave EPR and Fourier transform EPR. *Langmuir* 2004; **20**: 10238–10245.
19. Monaco V, Formaggio F, Crisma M, Toniolo C, Hanson P, Millhauser GL. Orientation and immersion depth of a helical

DOI: 10.1002/psc

lipopeptaibol in membranes using TOAC as an ESR probe. *Biopolymers* 1999; **50**: 239–253.
20. Toniolo C, Benedetti E. Structures of polypeptides from amino acids disubstituted at the α-carbon. *Macromolecules* 1991; **24**: 4004–4009.
21. Chan WC, White P (eds). *Fmoc Solid Phase Peptide Synthesis; A Practical Approach*. Oxford University Press: New York, 2000.
22. Marchetto R, Schreier S. Nakaie CRA novel spin-labeled amino acid derivative for use in peptide synthesis: (9-fluorenylmethyloxycarbonyl)-2,2,6,6-tetramethylpiperidine-N-oxyl-4-amino-4-carboxylic acid. *J. Am. Chem. Soc.* 1993; **115**: 11042–11043.
23. Nakaie CR, Silva EG, Cilli EM, Marchetto R, Schreier S, Paiva TB, Paiva ACM. Synthesis and pharmacological properties of TOAC-labeled angiotensin and bradykinin analogs. *Peptides* 2002; **23**: 65–70.
24. Whitmore L, Fallace BA. DICHROWEB, An online server for protein secondary structure analysis from circular dichroism spectroscopic data. *Nucleic Acids Res.* 2004; **32**: 668–673.
25. Schneider DJ, Freed JH. In *Biological Magnetic Resonance. Spin Labeling. Theory and Applications*, vol. 8, Berliner LJ, Reuben J (eds). Plenum Press: New York, 1989; 1–76.
26. Budil DE, Lee S, Saxena S, Freed JHJ. Nonlinear-least-squares analysis of slow-motion EPR spectra in one and two dimensions using a modified Levenberg-Marquardt algorithm. *Magn. Reson. A* 1996; **120**: 155–189.
27. Xu Y, Shen J, Luo X, Zhu W, Chen K, Ma J, Jiang H. Conformational transition of amyloid β-peptide. *Proc. Natl. Acad. Sci. U.S.A.* 2005; **102**: 5403–5407.
28. Rangachari V, Reed DK, Moore BD, Rosenberry TL. Secondary structure and interfacial aggregation of amyloid-beta(1–40) on sodium dodecyl sulfate micelles. *Biochemistry* 2006; **45**: 8639–8648.
29. Verdier Y, Zarandi M, Penke B. Amyloid beta-peptide interactions with neuronal and glial cell plasma membrane: binding sites and implications for Alzheimer's disease. *J. Pept. Sci.* 2004; **10**: 229–248.
30. Pike CJ, Walencewicz-Wasserman AJ, Kosmoski J, Cribbs DH, Glabe CG, Cotman CW. Structure-activity analyses of β-amyloid peptides: contributions of the β 25–35 region to aggregation and neurotoxicity. *J. Neurochem.* 1995; **64**: 253–265.
31. Terzi E, Holzemann G, Seelig J. Alzheimer β-amyloid peptide 25–35: electrostatic interactions with phospholipid membranes. *Biochemistry* 1994; **33**: 7434–7441.
32. Mandal PK, Pettegrew JW. Alzheimer's disease: NMR studies of asialo (GM1) and trisialo (GT1b) ganglioside interactions with Ab(1–40) peptide in a membrane mimic environment. *Neurochem. Res.* 2004; **29**: 447–453.
33. Shao H, Jao S, Ma K, Zagorski MG. Solution structures of micelle-bound amyloid beta-(1–40) and β-(1–42) peptides of Alzheimer's disease. *J. Mol. Biol.* 1999; **285**: 755–773.
34. Kallick DA, Tessmer MR, Watts CR, Li CY. The use of dodecylphosphocholine micelles in solution NMR. *J. Magn. Reson., B* 1995; **109**: 60–65.
35. Huibers PDT. Quantum-chemical calculations of the charge distribution in ionic surfactants. *Langmuir* 1999; **15**: 7546–7550.
36. Austen B, Christodoulou G, Terry JE. Relation between cholesterol levels, statins and Alzheimer's disease in the human population. *J. Nutr. Health Aging* 2002; **6**: 377–382.
37. Dante S, Hauβ T, Dencher NA. Cholesterol inhibits the insertion of the Alzheimer's peptide Aβ(25–35) in lipid bilayer. *Eur. Biophys. J.* 2006; **35**: 523–531.

DOI: 10.1002/psc